Int J Thermophys (2008) 29:261–270
DOI 10.1007/s10765-007-0343-3

Optimizing the Implementation of High-Temperature Fixed Points through the Use of Thermal Modeling

G. Machin · L. Wright · D. Lowe · J. Pearce

Published online: 24 January 2008

Abstract High-temperature fixed points (HTFP) have the potential to make a step-change improvement in high-temperature metrology, significantly reducing the uncertainty of scale realization of the current ITS-90 and improving dissemination of high-temperature scales to industry. However, in a practical implementation, the performance of HTFP could be limited, by, for example, injudicious use of insulation in the vicinity of the fixed point, furnace gradients, or incomplete filling. This article investigates some of these aspects for a selection of HTFP. Steady-state modeling of the influence of insulation on the radiance temperature was performed for Co–C (1,324°C), Pd–C (1,492°C), Pt–C (1,738°C), Ru–C (1,953°C), and Re–C (2,474°C) fixed points. This included studying mitigation scenarios through the insertion of different types and designs of insulation. The optimum design was identified to minimize the temperature drop in a particular furnace. It was found that, for the furnace and fixed-point combination modeled, the actual effect of the insulation was almost insignificant. Transient modeling was performed for a Re–C fixed point, to track the evolution of the radiance temperature through the melting transition. The starting point of the model was the beginning of the melt. The evolution of radiance temperature with time in "perfectly" filled cells was modeled with a range of linear temperature gradients across the eutectic cell. The gradient had a significant effect on the duration of the transition and on the structure of the melt itself. Despite the model's simplicity,

G. Machin (✉) · D. Lowe · J. Pearce
Division of Industry and Innovation, National Physical Laboratory, Teddington, Middlesex TW11 0LW, UK
e-mail: graham.machin@npl.co.uk

L. Wright
Division of Quality of Life, National Physical Laboratory, Teddington, Middlesex TW11 0LW, UK

it qualitatively demonstrated that the melt transition temperature, as identified by the point of inflection, could be significantly affected by the presence of furnace gradients.

Keywords Eutectics · High-temperature fixed points · Thermal modeling

1 Introduction

High-temperature fixed points (HTFP) based on the eutectic reaction of a pure metal (or a metal–carbide) and carbon have been the subject of intense study since they were first proposed [1,2]. An up-to-date survey of the current state of research is given in [3]. Within 10 years, it is envisaged that these fixed points will become established as primary references at high temperatures, be used to establish traceability to industry, and potentially form the basis of a future international temperature scale [4,5]. However, before full benefit can be taken from these new fixed points, several technical questions remain to be answered [5]. One of these is the effect of the furnace environment and, in particular, the influence, if any, that furnace temperature gradients have upon the measured temperature of the fixed point. The only realistic way to assess the effect of furnace environment is through thermal modeling. The work described in this article details thermal modeling that:

(a) calculates the temperature drop across the back wall for NPL-designed HTFP cells;
(b) investigates the effect of inserting insulation (e.g., graphite felt) in front of the radiating cavity (while leaving the radiating aperture unobstructed) on the temperature drop; and
(c) investigates the effect of furnace gradients on the melt.

The implications of these investigations are discussed in the context of practical implementation of HTFP. The results reported here were for non-contact thermometry fixed-point blackbody cells.

2 Construction of the Model

The model was constructed around the design of the HTFP and furnace of NPL [6]. Various assumptions were made to simplify the modeling process.

These assumptions were:

(a) The problem is axisymmetric.
(b) The heat transport by argon gas inside the furnace/fixed-point assembly was neglected. This is reasonable as radiation is by far the dominant heat transport mechanism at the temperatures of interest.
(c) For steady-state models, the region of the blackbody in contact with the eutectic is at the fixed-point temperature. This is certainly valid at the end of the melting process.
(d) For a given steady-state model, the thermal properties, in particular the thermal conductivity, of the graphite are constant. This is reasonable, given the very restricted range of temperatures over which each model was run.

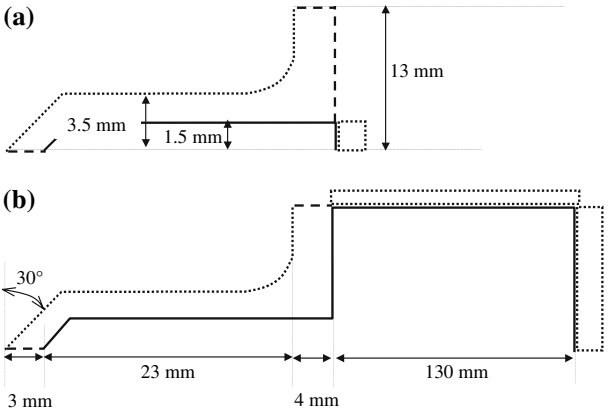

Fig. 1 Drawing of the blackbody model geometry (**a**) with no furnace and (**b**) with a furnace, indicating the types of boundary condition applied in different regions

The assumptions above mean that the steady-state models can be created that are effectively two-dimensional slices through the blackbody and furnace. Material properties were taken from [7]. The model is constructed as illustrated in Fig. 1. Two models are shown: one with a furnace and one without. Dotted lines are held at a fixed-point temperature. Solid lines are in radiative exchange with one another (some solid lines, e.g., the furnace and the outside world, are also at a fixed temperature). Dashed lines are assumed to be perfectly insulated. The outside world is held at 293 K throughout.

Models of two different furnaces were constructed; one was of a 100-mm long furnace held at the fixed-point temperature, the other was of a furnace 130 mm beyond the front of the blackbody with temperature gradients similar to those measured for the NPL furnace. Models were constructed with and without insulation, with baffles of different types, and the effect on the resultant temperature drop investigated.

Once the general description of the model had been developed, the finite element package Abaqus [8] was used to create a working version. This package was chosen, as it can handle radiation calculations within closed cavities and was able to solve the more general transient case. During initial trials, the model was run with increasingly finer finite-element meshes in order to ensure that the results were not affected by the mesh size. Once a suitable mesh was identified, it was used for all subsequent models.

3 Results of Modeling

The modeling took place in three stages. First, a steady-state model was constructed to calculate the temperature drop across the blackbody cavity back wall; second, the model was extended to include the heated furnace tube and investigations of gradients and the effect of baffles and insulation were undertaken; and, third, the model was further extended to include transient effects during the melting process. This was used to investigate the effects of imposed temperature gradients across the length of the cavity. The results of this modeling will be described in turn.

Table 1 Thermal properties of graphite and graphite felt used in modeling the high-temperature fixed points

Eutectic	Graphite felt thermal conductivity $\left(\mathrm{W \cdot m^{-1} \cdot K^{-1}}\right)$	Graphite thermal conductivity $\left(\mathrm{W \cdot m^{-1} \cdot K^{-1}}\right)$
Co–C	0.46	53.6
Pd–C	0.54	49.9
Pt–C	0.76	45.6
Ru–C	0.92	42.5
Re–C	1.32	36.6

Table 2 Comparison of modeled temperature drop between the results of equivalent models produced by Abaqus and previous work

	Previous work [9,10] (mK)			Abaqus model (this work, [13]) (mK)		
Eutectic	1.25 λ_{graph}	λ_{graph}	0.75 λ_{graph}	1.25 λ_{graph}	λ_{graph}	0.75 λ_{graph}
Co–C	10.5	13.0	17.0	10.5	13.2	17.5
Pd–C	16.5	21.0	27.0	16.8	21.0	27.8
Pt–C	29.0	38.0	50.0	30.9	38.5	51.2
Ru–C	49.0	60.0	80.0	49.5	61.8	82.1
Ir–C	96.0	113.0	150.0	95.8	119.2	158.1
Re–C	130.0	156.0	204.0	132.0	164.4	217.8

3.1 Calculation of the Temperature Drop Across the Back Wall

These calculations were undertaken to validate the model by comparison to previous results (using a different software package) given in [9,10]. A model was constructed, as closely identical as possible, to that reported in [9,10].

Three different conditions were then run:

1. a simple model with no furnace and the standard material property values for graphite (given in Table 1) at the fixed-point temperature (the dimensions of the cavity are given in [9,10]);
2. two models in which the thermal conductivity of graphite [λ_{graph}] was changed to 75% and to 125% of its usual value; and
3. a model including a 100-mm long furnace extension from the front of the fixed-point cavity, radius of 8 mm, uniformly held at the fixed-point temperature.

The results of these models are given in Table 2 (Models 1 and 2) and Table 3 (Model 3).

A comparison of the two models in Table 2 indicates good agreement with the previously published work; even the largest difference is less than 10%. Small differences can be attributed to differences in mesh details or in differences in the way the software packages solve the radiation transport problem. The agreement is sufficiently close

Table 3 Results of temperature drop values from models with a furnace, comparing previous results to Abaqus results using different furnace radii

Eutectic	Previous model 8 mm radius [9] (mK)	Abaqus 8 mm radius (mK)	Abaqus 10 mm radius (mK)
Co–C	10.5	9.3	11.4
Pd–C	16.8	14.8	18.1
Pt–C	30.5	27	33.1
Ru–C	49	43.3	53
Ir–C	94	82.8	101.5
Re–C	129	113.6	139.1

to consider that the model is validated, at least in the sense that it could adequately reproduce the results of the previous model.

The results of the third model are given in Table 3. Normal values for the thermal properties of graphite are used, i.e., the same as that used for λ_{graph} in Table 2. Two things are to be observed. First, by comparing this model to that in the previous table, the temperature drop is seen to be less than that of a freely radiating fixed point. This is to be expected as a proportion of the radiation lost from the back wall that is replenished from reflected radiation from the furnace walls. Second, the agreement between the previous model and the Abaqus models is not quite as good as the results presented in Table 2. It is thought that this is due to detailed differences in the way that the boundary conditions were imposed in the models; it can be seen, for instance, that the result is quite sensitive to small increases in radius.

3.2 Investigation of Effects of Insulation and Furnace Gradients on the Temperature Drop

With the model validated, heat flow within the cavity was investigated, and in particular how the introduction of baffles and insulation in the furnace in front of the radiating aperture affected the heat flow and resultant temperature drop. Figure 2 shows the steady-state model of the back-wall region of a Re–C fixed point in the absence of a furnace. The aperture of this cavity is 3 mm. As expected, the heat loss is predominantly from the back wall to the outside world—however, some heat loss is compensated by thermal radiation from the side wall (note arrows indicating direction of heat flux on the horizontal wall pointing right to left, i.e., toward the cavity back wall).

Several models of different fixed points were then constructed with different boundary conditions, namely, (a) a freely radiating fixed point (no furnace, no insulation), (b) a fixed point in a uniform furnace (i.e., no temperature gradient along its length) with no insulation, (c) a fixed point in a non-uniform furnace with no insulation, and (d) a fixed point in a non-uniform furnace with insulation. The non-uniformity of the furnace used to model the Re–C point of Fig. 3 was based on measured gradients, and similarly for the lower-temperature fixed points. The insulation, placed directly

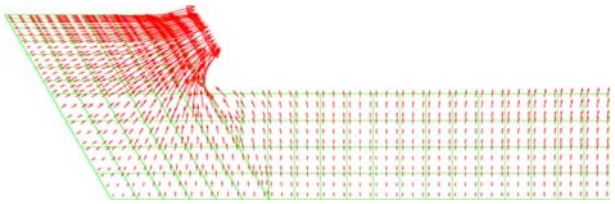

Fig. 2 Typical heat-flux vectors around the measurement region. The calculation is for Re–C, but would be the same for other high-temperature fixed points

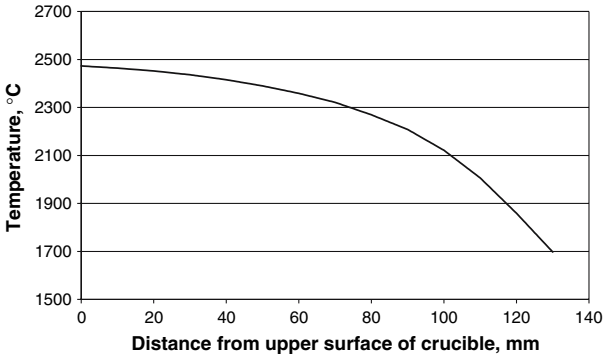

Fig. 3 Imposed furnace temperature gradient on model

Table 4 Temperature drops calculated from results of models with different furnace scenarios (all temperatures are given in mK)

Fixed-point metal	Co	Pd	Pt	Ru	Re
No furnace, no insulation	13.2	21	38.5	61.8	164
Uniform furnace, no insulation	11.4	18.3	33.4	53.5	141
Non-uniform furnace, no insulation	12	19.4	36	57.2	152
Non-uniform furnace, with insulation	10.7	17.4	32.3	51.1	136

in front of the aperture, was a 20 mm thick section of graphite felt, held in place by a 5-mm graphite block. A 3-mm aperture was made in the felt/graphite block combination to allow unrestricted viewing of the outside world by the fixed point. The thermal properties assumed for the graphite felt and graphite are given in Table 1. The results of the modeling are given in Table 4. The modeling indicates that, for small-aperture fixed points, the influence of thermal gradients, and even the presence of the furnace itself, have only a modest influence on the resultant predicted temperature drops. Also, the difference between a uniform and a non-uniform furnace and the role of insulation is limited, the effect being less than 100 mK at the highest temperatures. Of course, this effect would be significantly increased if larger-aperture fixed points were modeled.

3.3 Gradient Effects on the Resultant Temperature

To understand the effects of furnace temperature gradients on the temperature of the point of inflection of the fixed point, in this case a Re–C fixed point, a transient model was constructed. The results of this model will aid understanding of the contribution of temperature gradients to the overall uncertainty of the radiance temperature of these fixed points. The thermal conductivities of the solid and liquid phases of the Re–C alloy were assumed to be the same. To test the effects of this assumption, one model was run with the liquid thermal conductivity set at 90% that of the solid; this only affected the duration of the plateau. No mixing or convection effects were included in the model of the melting ingot. The latent heat of fusion was taken to be $177.7\,\mathrm{J}\cdot\mathrm{g}^{-1}$, and it was assumed that melting took place over the range from 2,747.15 to 2,748.15 K. One limitation of the model was that the effects of microstructure within the fixed point prior to melting were neglected. This is a significant limitation, and a point that will be returned to later in the discussion part of the article.

A two-dimensional axisymmetric finite-element model was constructed, using the same overall dimensions for the furnace and crucible as above. Simulations were then performed with the following imposed conditions:

(1) a transient model with crucible and a uniform furnace with insulation;
(2) a transient model with crucible and a uniform furnace;
(3) a transient model with the outer surface of the crucible at a uniform temperature; and
(4) a series of transient models where the crucible is stepped to +20 K above the nominal melting point of 2,747 K with the following gradients imposed on the crucible outer wall, pivoted at the crucible center,: −2 to +2 K, −5 to +5 K, −10 to +10 K, −15 to +15 K, +15 to −15 K, +10 to −10 K, +5 to −5 K, and +2 to −2 K.

The first two models were to quantify the effect of the insulation and furnace, and then just the furnace alone. The third model provided a baseline against which the models run in (4) were compared. The temperatures reported, as before, are the areal average over the region at the bottom of the blackbody cavity. The first three models yielded essentially the same result, indicating that, for the purpose of this model, the crucible alone could be modeled.

The results of (4) are shown in Fig. 4. As can be clearly seen, the point of inflection of the plateau does not change—this is to be expected for a single-component system whose plateau a priori is flat. However, the post-melt curve has structure and, critically, the break-off point of the melt moves significantly, i.e., its duration changes by up to 35%, dependent upon which gradient is imposed. If this thermal effect was imposed on a real binary (i.e., eutectic) system, then the fixed-point temperature, as determined by the point of inflection, would definitely change.

4 Discussion

Thermal modeling has been used to estimate the temperature drop across the back wall of the NPL fixed-point cavities. The results were in good agreement with those of

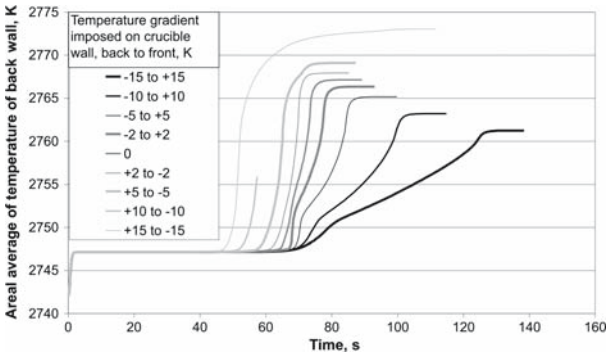

Fig. 4 Results of transient modeling with linear temperature gradient across the crucible. The crucible was held 20 K above the melting point and then the following gradients were imposed: m15 was −15 K to +15 K, m10 was −10 K to +10 K . . . to p15 was +15 K to −15 K. *x*-axis is time in arbitrary units, *y*-axis is radiance temperature in K

other researchers [9,10]. The model constructed here could be used both to estimate the temperature drop and to investigate its sensitivity to different parameters, such as uncertainties in graphite thermal conductivity, emissivity at high temperatures [11], or dimensional inaccuracies. In particular, the model showed that the temperature drop was quite sensitive to input parameters (e.g., 30% for a reasonable range of graphite thermal-conductivity values). However, its *actual* value was quite small, for this design of fixed points, and it could be reasonably incorporated into the fixed-point uncertainty budget rather than applying a correction. However, note that the situation might well be radically different for large-area cavities where much larger temperature drops will be encountered [9,10].

Optimization of experimental design can be augmented by the use of thermal modeling. Previously, researchers have included graphite baffles and graphite insulation, including felt and foil, in an attempt to negate furnace gradients. The model constructed here allows the rigorous investigation of the effect of this furnace architecture on the temperature drop. As can be seen by comparing the values for Re–C in Table 4, for this design of a fixed point, there is only a small improvement due to the use of insulation. This is best illustrated by considering the Re–C point results in Table 4. The first entry is the reference worst case, a "bare" crucible freely radiating with no furnace in place. The second model included a uniform furnace, and this improved the temperature drop by just over 20 mK. The third model was for a non-uniform furnace, while the fourth model was a non-uniform furnace with insulation—the insulation resulted in a nearly 20 mK improvement to the temperature drop. It can be inferred that if a uniform temperature furnace with insulation had been modeled, the improvement would have been similar. It can, therefore, be deduced that (a) a uniform furnace is important to minimize the temperature drop and that (b) the use of insulation can effect further improvements. However, the most important thing to note here is that, for this design of blackbody, the temperature drop is quite insensitive to furnace conditions, provided the furnace temperature is uniform over the crucible. This is a priori

the case during a phase transition, and can be assisted during the heating and cooling cycles by including pyrolytic graphite liners [12].

Transient modeling of a fixed point through a melt yielded valuable information about both the thermal gradients within the furnace and also the possible contribution that thermal gradients might make to the temperature, if it is defined by the point of inflection (Fig. 4). The "post-melt" curve has structure in it, particularly for the models where the gradient is higher at the front of the crucible and lower at the back. This structure, particularly the slow rise out of the melt, indicates that the melt front is not uniform and that there is break-through of molten material onto the blackbody tube well before all the fixed-point material is melted. The "post-melt" kink is probably due to the final melting of the remaining portion of ingot surrounding the back wall. This structure is not seen in the models where the furnace gradient is reversed—i.e., hotter at the back than at the front—although the melt duration is significantly reduced.

These curves can give some indication to users as to which type of gradients they might have in their furnace and might suggest mitigation strategies, particularly if slow rises out of melts and kinks in the post-melts are present. The limitation of this model is that the eutectic is treated as a single system and, hence, has a flat plateau. This is not the case for a non-equilibrium system like a eutectic which has intrinsic structure in the pre-melt ingot. This internal energy leads to "pre-melting" and a non-flat plateau. If the effects observed in the model are present, and the temperature of the fixed-point is determined by the point of inflection, then a different temperature might result, depending upon the quality of the furnace. This is because the fully melted condition is achieved much more rapidly for some furnace gradients than others, causing premature ending of the melt and shifting the point of inflection to potentially lower temperatures. Although the point of inflection is stable and the reliable determination of temperature in good (i.e., uniform) furnaces is relatively simple, it is probably not the best general approach for determining high-temperature fixed-point temperatures. The method proposed in [13], which involves extrapolation to zero solid fraction, may well provide a more robust approach in the longer term.

5 Conclusions

Thermal modeling has been used to optimize the design of high-temperature measurement experiments. It has been used to make inferences of the general thermal conditions in a high-temperature furnace and to estimate possible corrections due to the temperature drop and indicate how estimates of one component of high-temperature fixed-point radiance temperature uncertainty might be determined.

Acknowledgments This work was supported by the UK Department of Trade and Industry Software Support for Metrology Project SSfM3.1.2.1 and Thermal Programme Contract Number: GBBK/C/13/17.

References

1. Y. Yamada, H. Sakate, F. Sakuma, A. Ono, Metrologia **38**, 213 (2001)
2. N. Sasajima, Y. Yamada, H. Sakuma, in *Temperature: Its Measurement and Control in Science and Industry*, vol. 7, ed. by D.C. Ripple (AIP, New York, 2003), pp. 279–284

3. E. Woolliams, G. Machin, D. Lowe, R. Winkler, Metrologia **43**, R11 (2006)
4. G. Machin, A paradigm change in high temperature metrology. *Invited review paper to IMEKO World Congress*, Rio de Janeiro, Brazil (Sept 2006)
5. G. Machin, P. Bloembergen, J. Hartmann, M. Sadli, Y. Yamada, in *Proceedings of TEMPMEKO 2007*, Int. J. Thermophys. **28**, 1976 (2007), DOI: 10.1007/s10765-007-0250-7
6. D.H. Lowe, G. Machin, *Proceedings of SICE Annual Conference*, Sapporo, Japan, 2004, pp. 802–806
7. Y.S. Touloukian, R.W. Powell, C.Y. Ho, P.G. Klemens, *The TPRC Data Series*, vol. 2 (Plenum Press, New York, 1978)
8. http://www.abaqus.com/products/products_overview.html
9. P. Jimeno-Largo, Ph.D. Thesis, University of Valladolid, 2007
10. P. Jimeno-Largo, Y. Yamada, P. Bloembergen, M.A. Villamanan, G. Machin, in *Proceedings of TEMPMEKO 2004, 9th International Symposium on Temperature and Thermal Measurements in Industry and Science*, ed. by D. Zvizdić, L.G. Bermanec, T. Veliki, T. Stašić (FSB/LPM, Zagreb, Croatia, 2004), pp. 335–340
11. T.J. Esward, L. Wright, *Software Support for Metrology Good Practice Guide 15: Continuous Modeling* (March 2006), http://www.npl.co.uk/ssfm/download/
12. Y. Yamada, B. Khlevnoy, Y. Wang, T. Wang, K. Anhalt, Metrologia **43**, S140 (2006)
13. D. Lowe, K. Mingard, Z. Malik, P. Quested, in *Proceedings of TEMPMEKO 2007*, Int. J. Thermophys. **28**, 2019 (2007), DOI: 10.1007/s10765-007-0290-z